ELSEVIER

Engineering Analysis with Boundary Elements 30 (2006) 940–948

ENGINEERING ANALYSIS with BOUNDARY ELEMENTS

www.elsevier.com/locate/enganabound

Dual BIE approaches for modeling electrostatic MEMS problems with thin beams and accelerated by the fast multipole method

Y.J. Liu*

Department of Mechanical, Industrial and Nuclear Engineering, University of Cincinnati, P.O. Box 210072, Cincinnati, OH 45221-0072, USA

Received 9 January 2006; accepted 18 April 2006
Available online 7 September 2006

Abstract

Three boundary integral equation (BIE) formulations are investigated for the analysis of electrostatic fields exterior to thin-beam structures as found in some micro-electro-mechanical systems (MEMS). The three BIE formulations are: (1) the regular BIE using only the single-layer potential; (2) the dual BIE (a) using the regular BIE on one surface of a beam and the gradient BIE on the other surface; and (3) the dual BIE (b) using a linear combination of the regular BIE and gradient BIE on all the surfaces of the beam. Similar to crack problems in elasticity, the regular BIE degenerates when the beam thickness tends to zero, while the two dual BIE formulations do not degenerate. Most importantly, the dual BIE (b) is found to be well conditioned for all the values of the beam thickness, and thus well suited for implementation with the fast multipole BEM. The fast multipole BEM for both the regular BIE and the dual BIE (b) formulations are developed and tested on a simplified comb-drive model. The numerical results clearly show that the dual BIEs are very effective in solving MEMS problems with thin beams and the fast multipole BEM with the dual BIE (b) formulation is very efficient in solving large-scale MEMS models.
© 2006 Published by Elsevier Ltd.

Keywords: Fast multipole method; Boundary element method; Electrostatic problems; MEMS

1. Introduction

Boundary integral equation (BIE) formulations and their numerical solutions using the boundary element method (BEM) [1–5] are well suited for the analyses of the thermal, electrical and mechanical fields in micro-electro-mechanical systems (MEMS), because of the advantages of the BEM in handling complicated geometries and infinite domain problems. Some of the early work using the BEM for modeling MEMS problems include papers in [6–8] for electrostatic analysis of fields exterior to MEMS structures, in [9] for dynamic analysis and in [10] for coupled mechanical-electrical analysis. Most recently, a thin-beam BIE (in 2-D) and a thin-plate/shell BIE (in 3-D) for the electrostatic analysis of MEMS problems have been proposed in [11,12], with the analogy to the crack problems in elasticity. These thin-beam and thin-plate/shell BIEs only need to model one surface of such structures with the BEM and thus are very efficient in analyzing complicated MEMS problems with very thin structures. Modeling MEMS problems using 2-D models has limited applications, but can be applied in preliminary studies of the MEMS problems if the fields are mainly confined in a 2-D space. The works in [12–14] are some recent examples in solving the electrostatic fields using the BIEs for 2-D models.

Analysis of MEMS problems often requires large models that can accurately predict the rapidly changing fields surrounding complicated structures. The conventional BEM approach requires $O(N^3)$ operations to solve the BEM system using direct solvers (with N being the number of equations) or $O(N^2)$ operations using iterative solvers. Thus the conventional BEM is often found inefficient in solving large-scale problems with the number of equations above a few thousands. The fast multipole method (FMM) [15–17] and other fast methods can be used to accelerate the solutions of the BEM by several folds, promising to reduce the CPU time and memory usage in the fast multipole accelerated BEM to $O(N)$. A comprehensive

*Tel.: +1 513 556 4607; fax: +1 513 556 3390.
E-mail address: Yijun.Liu@uc.edu.

0955-7997/$ - see front matter © 2006 Published by Elsevier Ltd.
doi:10.1016/j.enganabound.2006.04.010

review of the fast multipole accelerated BEM can be found in Ref. [18]. Applications of the fast multipole and other related fast BEM approaches for modeling MEMS problems can be found in [19–21] using the FMM and in [22,23] using the precorrected-FFT method.

In this paper, three BIE formulations are investigated for the analysis of electrostatic fields exterior to thin-beam structures as found in MEMS problems, including: (1) the regular BIE; (2) the dual BIE (a) using the regular BIE on one surface of the beam and the gradient BIE on the other surface; and (3) the dual BIE (b) using a linear combination of the regular BIE and gradient BIE on all surfaces of the beam. Compared with the thin-beam BIE [12] where only one surface needs to be discretized using boundary elements, the dual BIE approaches need to solve systems of equations that are twice as large as in using the thin-beam BIE. However, separate charge densities can be obtained directly from the BEM equations using the dual BIE formulations and no additional post-processing needs to be performed in order to obtain the charge densities. The FMM is used to accelerate the dual BIE solutions and the larger system of equations does not present any difficulties in modeling MEMS problems.

In the literature, a dual BIE approach has been applied in [14] to MEMS problems for estimating the errors in the BEM solutions and for directly computing the tangential electric field. A dual BIE formulation has also been proposed in [21,24] for evaluating damping forces due to Stokes flows in MEMS problems. To the author's best knowledge, the suitability of the dual BIEs for modeling electrostatic problems in MEMS with thin beams and their combinations with the fast multipole BEM have not been reported in the literature.

This paper is organized as follows: in Section 2, the three BIE formulations for 2-D electrostatic problems are reviewed. In Section 3, the fast multipole BEM for these electrostatic BIEs are presented. In Section 4, numerical examples are presented to demonstrate the effectiveness of the BIEs for thin-beam problems and the efficiencies of the fast multipole BEM for large-scale MEMS problems. The paper concludes with some discussions in Section 5.

2. The BIE formulations

Consider a 2-D infinite domain V embedded with many thin electric conductors (Fig. 1). The electric potential ϕ in V satisfies the Laplace equation and can be given by using the following representation integral:

$$\phi(\mathbf{x}) = \int_S \left[\frac{1}{\varepsilon} G(\mathbf{x},\mathbf{y})\sigma(\mathbf{y}) - \frac{\partial G(\mathbf{x},\mathbf{y})}{\partial n(\mathbf{y})}\phi(\mathbf{y})\right] \mathrm{d}S(\mathbf{y}) + C, \quad \forall \mathbf{x} \in V, \tag{1}$$

where $S = \cup S_\alpha$ is the boundary of V, ε the dielectric constant, $G(\mathbf{x},\mathbf{y})$ the Green's function given by

$$G(\mathbf{x},\mathbf{y}) = \frac{1}{2\pi}\ln\left(\frac{1}{r}\right), \quad \text{with} \quad r = |\mathbf{x}-\mathbf{y}|. \tag{2}$$

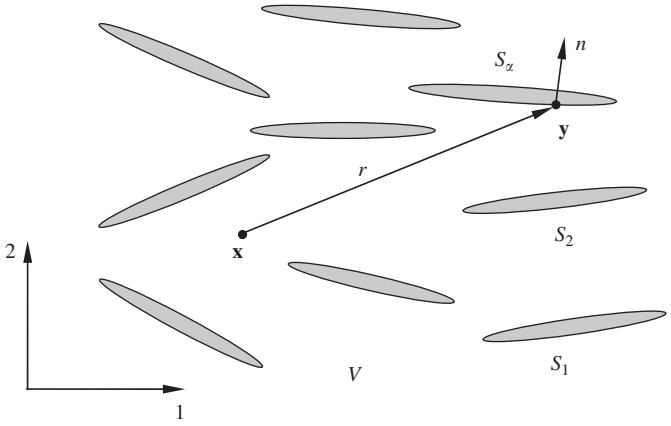

Fig. 1. A domain V embedded with many thin electric conductors.

σ the charge density defined by

$$\sigma(\mathbf{y}) \equiv \varepsilon \frac{\partial \phi}{\partial n}(\mathbf{y}), \tag{3}$$

with n being the outward normal, and C a constant representing the potential at infinity. If the potential on each conductor is kept constant (with applied voltage), the integral of the second term in Eq. (1) vanishes due to the properties of the kernel (see, e.g., Ref. [25]) and Eq. (1) is reduced to

$$\phi(\mathbf{x}) = \frac{1}{\varepsilon}\int_S G(\mathbf{x},\mathbf{y})\sigma(\mathbf{y})\,\mathrm{d}S(\mathbf{y}) + C, \quad \forall \mathbf{x} \in V \cup S, \tag{4}$$

where the source point $\mathbf{x}$ can be placed on the boundary S directly due to the smoothness of the G kernel. Eq. (4) with $\mathbf{x} \in S$ is called the *regular BIE* in Ref. [12].

Taking the derivative of Eq. (4) with $\mathbf{x} \in V$ and then letting $\mathbf{x}$ go to the boundary, one obtains the following *gradient BIE* [12]:

$$\frac{1}{2}\sigma(\mathbf{x}) = \int_S F(\mathbf{x},\mathbf{y})\sigma(\mathbf{y})\,\mathrm{d}S(\mathbf{y}), \quad \forall \mathbf{x} \in S \tag{5}$$

for smooth boundary S, in which the singular kernel F is given by

$$F(\mathbf{x},\mathbf{y}) = \frac{\partial G(\mathbf{x},\mathbf{y})}{\partial n(\mathbf{x})}. \tag{6}$$

Note that Eq. (5) is a homogeneous equation and cannot be applied alone to solve for the charge density on the surfaces directly. In fact, the system of equations using BIE (5) must be singular in general, otherwise one can always conclude that $\sigma = 0$ on the boundary.

In Ref. [12], a thin-beam BEM approach is developed based on the regular BIE (4) and gradient BIE (5) by taking the limit as the thickness of the beam tends to zero. In the limit as the two main surfaces of a beam become close to each other, BIE (4) degenerates and thus cannot be used to solve for the charge densities on the top and bottom surfaces separately. However, the thin-beam regular BIE from (4) can be applied to solve for the sum

of the charge densities on the top and bottom surfaces of each beam and the thin-beam gradient BIE from (5) can be applied to determine the separate charges in a post processing stage [12]. The thin-beam BEM based on this approach is very efficient for thin-beam models (e.g., with the thickness to length ratio of a beam $h/L \leqslant 0.001$), since only one surface needs to be discretized for each beam.

In this paper, a different approach is proposed to modeling MEMS with thin beams. As shown in Fig. 1, those thin beam like conductors are similar to open cracks (when the beam thickness is small but finite) or true cracks (when the beam thickness is approaching zero) in elasticity problems. For crack problems, the dual BIE (or composite BIE) approaches combining the regular BIE and gradient BIE have been proven to be very effective [26,27]. The advantages of using the dual BIE approaches are that they are valid for both open crack and true crack cases, without the need to switch the BIE formulations, and the original boundary variables can be solved directly. Because of the similarities mentioned above, the dual BIE approaches should be equally effective in solving electrostatic problems with thin beams (inclusions). The following two dual BIE formulations are tested in this study and both are found to be effective for modeling MEMS with thin beams.

(a) *Dual BIE (a)*: In this approach, the regular BIE (4) is applied on the top and edge surfaces of a beam while the gradient BIE (5) is applied on the bottom surface of the beam [26,27]. The disadvantage of this approach is that the coefficients are not uniform regarding their orders of magnitudes, since part of them are from the regular BIE and the other part from the gradient BIE which has a different order of singularity.

(b) *Dual BIE (b)*: In this approach, a linear combination of the regular BIE and gradient BIE is applied on the entire surfaces of the domain (all the beams), in the form:

$$\alpha(\text{regular BIE}) + \beta(\text{gradient BIE}), \tag{7}$$

where α and β are two constants. The selection of the parameters α and β is crucial for the performance of the dual BIE (b). In general, β should be smaller relative to α, so that the gradient BIE will not dominate in this dual BIE formulation. In this study of MEMS problems with thin beams, the choice of $\alpha = 1$ and $\beta = h_0 - h$ has been found to be sufficient, with h_0 being a reference thickness and h the thickness of the beam. For acoustic problems, Eq. (7) is the Burton–Miller BIE formulation that is very effective in overcoming the fictitious eigenfrequency difficulties for exterior acoustic problems (see, e.g., [28,29]). The advantage of this linear combination is that the same BIE formulation is applied uniformly over the entire boundary and thus better conditioning can be expected, as will be shown in this paper.

Both conventional BEM and fast multipole BEM codes based on the above BIE formulations have been developed in this study. For constant elements (line segments), both the G and F integrals in BIEs (4) and (5) can be integrated analytically, for all non-singular, nearly singular, or singular cases. Thus, the codes can handle very thin beams with very small but finite thickness or small gaps in the MEMS models, without any difficulties regarding the nearly singular or singular integrals.

3. The FMM

The FMM can be employed to accelerate the BEM for solving Eqs. (4) or (7). The main idea of the FMM is to translate the node-to-node (or element-to-element) interactions to cell-to-cell interactions using various expansions and translations. Iterative equation solvers (such as GMRES) are used in the FMM, where matrix–vector multiplications are calculated using fast multipole expansions. Using the FMM for the BEM, both the solution time and memory requirement for solving a problem can be reduced to order $O(N)$, with N being the total number of unknowns.

The fast multipole BEM for 2-D potential problems has been well documented (see, e.g., Refs. [17,18,30]). For completeness, the main results for the G kernel integral in BIE (4) are summarized first. Then the treatment of the F kernel integral in BIE (5) is discussed.

The G kernel in BIE (4) can be represented by complex variables as [17,18,30]:

$$G(z_0, z) = -\frac{1}{2\pi}\ln(z_0 - z) = \frac{1}{2\pi}\sum_{k=0}^{\infty} O_k(z_0 - z_c) \times I_k(z - z_c), \tag{8}$$

in which $z_0 = x_1 + ix_2$ and $z = y_1 + iy_2 (i = \sqrt{-1})$ represent $\mathbf{x}$ and $\mathbf{y}$, respectively, z_c is an expansion point close to z, and the two auxiliary functions are defined by

$$I_k(z) = \frac{z^k}{k!}, \quad \text{for } k \geqslant 0,$$

$$O_k(z) = \frac{(k-1)!}{z^k}, \quad \text{for} \quad k \geqslant 1; \quad \text{and}$$

$$O_0(z) = -\ln(z).$$

The integral in the regular BIE (4) can be evaluated using the *multipole expansion*:

$$\int_{S_0} G(z_0, z)\sigma(z)\,\mathrm{d}S(z) = \frac{1}{2\pi}\sum_{k=0}^{\infty} O_k(z_0 - z_c)M_k(z_c), \tag{9}$$

where S_0 is a subset of S away from $\mathbf{x}$, and the *moment* about z_c is

$$M_k(z_c) = \int_{S_0} I_k(z - z_c)\sigma(z)\,\mathrm{d}S(z). \tag{10}$$

If the expansion point z_c is moved to a new location $z_{c'}$, one has the following *M2M translation* for the moments:

$$M_k(z_{c'}) = \sum_{l=0}^{k} I_{k-l}(z_c - z_{c'})M_l(z_c). \tag{11}$$

Let z_L be a point close to z_0, one can have the following *local expansion*:

$$\int_{S_0} G(z_0,z)\sigma(z)\,\mathrm{d}S(z) = \sum_{l=0}^{\infty} L_l(z_L) I_l(z_0 - z_L), \tag{12}$$

where the coefficients are given by the following *M2L translation*:

$$L_l(z_L) = \frac{(-1)^l}{2\pi} \sum_{k=0}^{\infty} O_{l+k}(z_L - z_c) M_k(z_c). \tag{13}$$

If the point for local expansion is moved from z_L to $z_{L'}$, one has the following *L2L translation*:

$$L_l(z_{L'}) = \sum_{m=l}^{\infty} I_{m-l}(z_{L'} - z_L) L_m(z_L). \tag{14}$$

Now consider the integral with the F kernel in the gradient BIE (5):

$$\int_{S_0} F(z_0,z)\sigma(z)\,\mathrm{d}S(z) = \int_{S_0} \frac{\partial G(z_0,z)}{\partial n(z_0)} \sigma(z)\,\mathrm{d}S(z), \tag{15}$$

which is different from the F kernel integral in Ref. [30] where the normal derivative is at the field point z. There are two ways to handle this integral. One way is to shift the derivative to the field point and introduce a new moment. Then all the *M2M*, *M2L*, and *L2L* translations will be the same as given above. However, it is found that this approach requires additional memory for storing the new moment. Another way to handle this integral is to keep the derivative at the source point and apply the same moment as used for the G kernel integral. In this way, no new moment need to be stored and only the *M2L* translation need to be modified. This approach is used in this study and discussed in the following.

$F(z_0, z)$ can be expressed as

$$F(z_0,z) = \frac{\partial G(z_0,z)}{\partial n(z_0)} = (n_1 + in_2)(z_0) G' = n(z_0) G', \quad \text{with} \quad G' \equiv \frac{\partial G}{\partial z_0}. \tag{16}$$

One has from Eq. (8):

$$G' = -\frac{1}{2\pi} \sum_{k=0}^{\infty} O_{k+1}(z_0 - z_c) I_k(z - z_c). \tag{17}$$

Thus the *multipole expansion* for the F kernel integral in BIE (5) can be given by

$$\int_{S_0} F(z_0,z)\sigma(z)\,\mathrm{d}S(z) = -\frac{1}{2\pi} n(z_0) \sum_{k=0}^{\infty} O_{k+1}(z_0 - z_c) M_k(z_c), \tag{18}$$

where $M_k(z_c)$ is the same moment as given in Eq. (10).

It can also be shown that the *M2M* and *L2L* translations and the local expansion for the F kernel integral remain the same as for the G kernel integral, except that the *M2L* translation is changed to:

$$L_l(z_L) = \frac{(-1)^{l+1}}{2\pi} n(z_0) \sum_{k=0}^{\infty} O_{l+k+1}(z_L - z_c) M_k(z_c). \tag{19}$$

The fast multipole BEM is implemented for both the regular BIE and dual BIE (b) formulations based on the fast multipole BEM code presented in Ref. [30]. The procedures and implementation details of the fast multipole BEM based on the above expansions and translations are similar to those for the general 2-D potential problems, which can be found in Ref. [30]. For constant elements, the moments can be evaluated analytically and thus no numerical integrations are used for the fast multipole BEM in this study.

4. Numerical examples

Numerical examples are presented to demonstrate the effectiveness and accuracy of the dual BIE formulations for electrostatic analysis of thin beam problems and the efficiency of the fast multipole BEM for modeling 2-D MEMS models.

(a) *Two parallel beam models using the three BIE formulations and conventional BEM*: A two parallel beam model (Fig. 2) suggested in Ref. [12] (in which $d = 0$) is considered first to verify the BIE formulations using the conventional BEM. The length of the beam is L, thickness is h, and gap between the beams is g. An offset d in the x direction may also be introduced between the two beams (Fig. 2). A potential V is applied to the top beam, while the negative potential $(-V)$ applied to the bottom beam. For this problem, the analytical solution for the charge density σ^- on the lower surface of the top beam (Fig. 2) is given by (see, e.g., Ref. [31]):

$$\sigma^- = \varepsilon \frac{\partial \phi}{\partial n} = \varepsilon \frac{\Delta V}{\Delta n} = \varepsilon \frac{2V}{g}, \tag{20}$$

for the region away from edges of the beams. This formula is used to verify the BEM results.

One model, with the parameters $\varepsilon = 1$, $L = 0.01\,\mathrm{m}$, $h = 0.0001\,\mathrm{m}$, $g = 0.0011\,\mathrm{m}$, $d = 0$, $V = 1$, $C = 0$, is tested first with the regular BIE, dual BIE (a) and dual BIE (b)

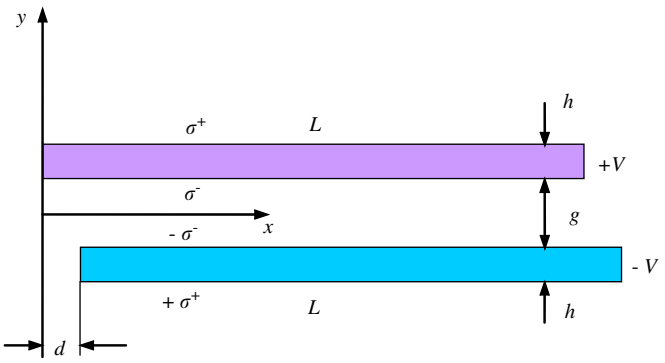

Fig. 2. A two parallel beam model for testing the BIE formulations.

and solved with the conventional BEM using constant elements. The number of elements along the beam length direction is increased from 10, 20, 50, to 100, while 5 elements is used on each edge (side) of the beams, corresponding to BEM models with 30, 50, 110, and 210 elements per beam, respectively. The BEM results using the three BIE formulations converged very quickly. Fig. 3 shows the convergence of the BEM results using the dual BIE (b) for the charge densities on the lower and upper surfaces of the top beam (Fig. 2). In fact, the model with just 10 elements along the beam length direction yields a value of σ^- at the middle of the lower surface of the top beam that agrees with the analytical solution ($\sigma^- = 1818$ in this case) within the first four digits. With the increases of the elements along the beam length direction, only results near the two edges of the beam change, tending to infinity due to the singularity of the field at the edges [12].

Fig. 4 shows the charge density on the top beam in the same parallel beam model, but with an offset $d = g = 0.0011$ m, and using 210 elements per beam. The charge densities in the middle of the beam remain the same ($\sigma^- = 1818$) while the fields near the edges have marked changes. The charge densities on the bottom beam (Fig. 2) have negative values and are "anti-symmetrical" relative to the results on the top beam and thus are not plotted.

The effectiveness of the dual BIE formulations in solving cases with extremely thin beams is demonstrated next. Table 1 is the comparison of the charge densities on the top beam in the two-beam model with a different set of parameters ($\varepsilon = 1$, $L = 0.01$ m, $g = 0.001 + h$, $d = 0$, $V = 1$, $C = 0$, and 210 elements per beam). The ratio h/L is changed from 0.1 to 10^{-16}. The regular BIE (Eq. (4)) works very well until the ratio h/L reaches 10^{-8}, after which the regular BIE degenerates for thin-beam problems. The high accuracy of the regular BIE is most likely contributed by the analytical integration of all integrals,

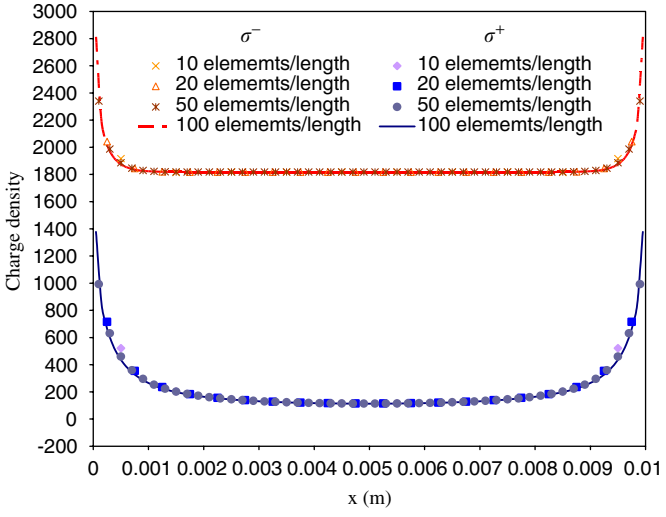

Fig. 3. Convergence of the BEM results using dual BIE (b) on the top beam in the parallel beam model ($\varepsilon = 1$, $L = 0.01$ m, $h = 0.0001$ m, $g = 0.0011$ m, $d = 0$, $V = 1$, $C = 0$).

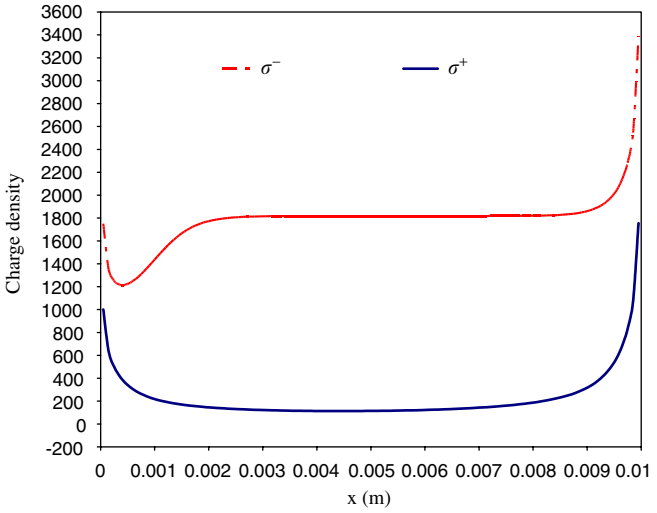

Fig. 4. Charge density on the top beam in the parallel beam model with offset ($\varepsilon = 1$, $L = 0.01$ m, $h = 0.0001$ m, $g = 0.0011$ m, $d = g$, $V = 1$, $C = 0$, 210 elements per beam).

Table 1
Comparison of the charge densities on the top beam in the two-beam model ($\varepsilon = 1$, $L = 0.01$ m, $g = 0.001 + h$, $d = 0$, $V = 1$, $C = 0$, 210 elements per beam)

H/L	Regular BIE		Dual BIE (a)		Dual BIE (b)		Analytical solution
	σ^-	σ^+	σ^-	σ^+	σ^-	σ^+	σ^-
1.0E−1	1000	95.18	1000	95.21	1000	95.18	1000
5.0E−2	1333	103.0	1333	103.0	1333	103.4	1333
1.0E−2	1818	112.0	1818	112.0	1818	113.0	1818
5.0E−3	1905	113.5	1905	113.5	1905	114.8	1905
1.0E−3	1980	114.9	1980	114.9	1980	115.9	1980
1.0E−4	1998	115.4	1998	115.4	1998	115.7	1998
1.0E−5	2000	115.5	2000	115.5	2000	115.6	2000
1.0E−6	2000	115.5	2000	115.5	2000	115.6	2000
1.0E−7	2000	115.5	2000	115.5	2000	115.6	2000
1.0E−8	2003	114.5	2000	115.5	2000	115.6	2000
1.0E−9	—	—	2000	115.6	2000	115.6	2000
1.0E−10	—	—	2000	115.6	2000	115.6	2000
1.0E−11	—	—	2000	115.6	2000	115.6	2000
1.0E−12	—	—	2000	115.6	2000	115.6	2000
1.0E−13	—	—	2000	115.7	2000	115.6	2000
1.0E−14	—	—	2000	115.2	2000	115.6	2000
1.0E−15	—	—	—	—	2000	115.6	2000
1.0E−16	—	—	—	—	2000	115.6	2000

which also likely delays the onset of the degeneracy of the regular BIE for thin-beam models. The dual BIE (a) (with regular BIE (4) collocating on the upper surfaces and edges, and gradient BIE (5) on the lower surfaces) and dual BIE (b) (with the linear combination (7) on all surfaces) work extremely well until the ratio h/L reaches 10^{-14} and 10^{-16}, respectively. After $h/L = 10^{-16}$, the double precision used in the code breaks down in representing the small values. It should be pointed out that the exercise done here is for pure investigation of the mathematical behaviors of the regular BIE and dual BIE formulations in the extreme

cases when the thickness of a beam approaches zero. In real MEMS applications, $h/L = 10^{-16}$ may never be practical.

The condition numbers of the BEM systems of equations using the three BIE formulations for the above cases are plotted in Fig. 5. As expected, the condition numbers for the system with the regular BIE increase quickly as the thickness of the beams decrease, which indicates that the regular BIE is towards degeneracy for thin-beam problems. The condition numbers for the dual BIE (a) also increase to such a high level that the reliability of the results is in question. This may be an indication of the poor conditioning of the BEM equations caused by the mismatch in the magnitudes of the coefficients from the G kernel and those from the F kernel. The condition numbers for the dual BIE (b) stay almost at a constant level as the thickness decreases, reflecting the good conditioning of the systems using the dual BIE (b) which produces a more uniform distribution of the coefficients. For the fast multipole BEM, good conditioning of a system is very important in ensuring the convergence of the solutions by iterative solvers. Thus, the dual BIE (b), that is valid for both thick or extremely thin beam models, seems to be an ideal candidate to be used with the fast multipole BEM.

(b) *Comb-drive models using the fast multipole BEM*: A simplified comb-drive model is studied next using the developed fast multipole BEM and compared with the conventional BEM which uses a direct solver (LAPACK) for solving the linear system. For the fast multipole BEM, the numbers of terms for both moments and local expansions are set to 15, the maximum number of elements in a leaf to 100, and the tolerance for convergence of the solutions to 10^{-6}. All the computations were done on a Pentium IV laptop PC with a 2.4 GHz CPU and 1 GB RAM.

The comb-drive models are built with the basic two parallel beam model shown in Fig. 2. The parameters used are $\varepsilon = 1$, $L = 0.01$ m, $h = 0.0002$ m, $g = 0.0003$ m, $d = 0.0005$ m, $V = 1$, $C = 0$. Fig. 6 shows a model with 17 beams (fingers). The two support beams on the left and right sides in Fig. 6 are not modeled in the BEM discretization. Two hundred elements are used along the beam length and 5 elements on each edge (with a total of elements equal to 410 for each beam). When more beams

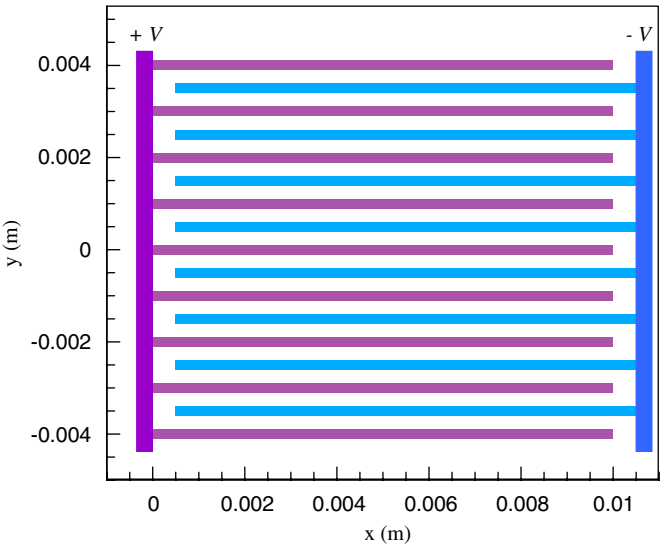

Fig. 6. A 2-D comb-drive model with 17 beams.

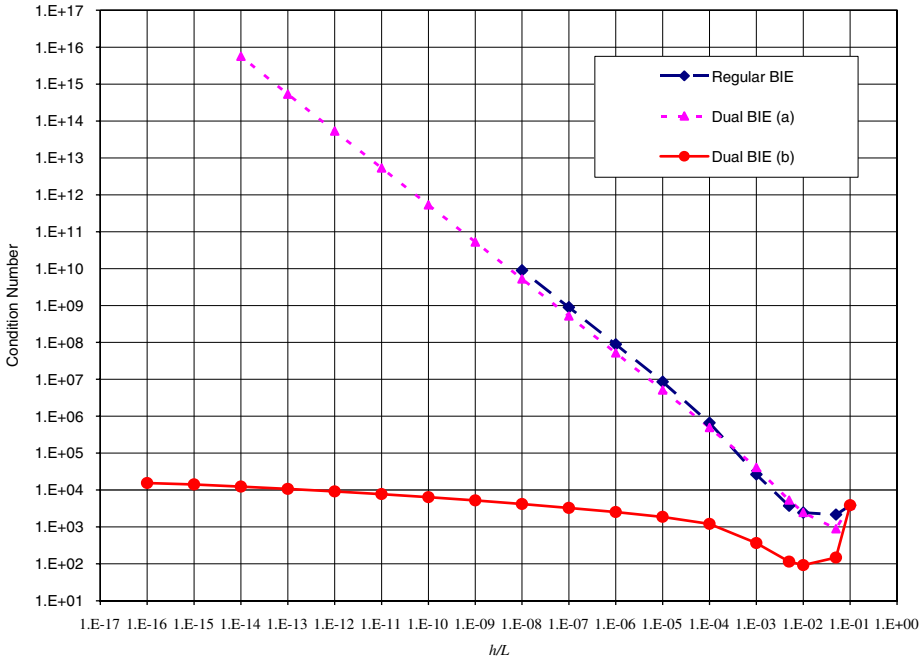

Fig. 5. Condition numbers of the systems of equations using the different BIE formulations.

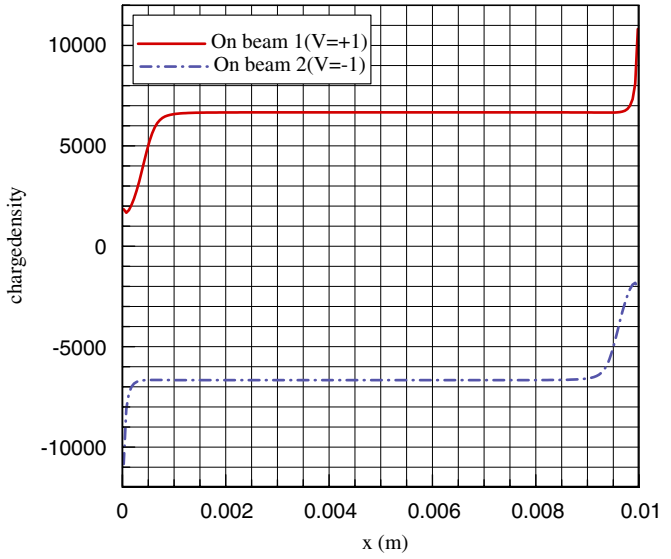

Fig. 7. Charge densities on the center beam 1 and beam 2 (below the center beam) (Fig. 6).

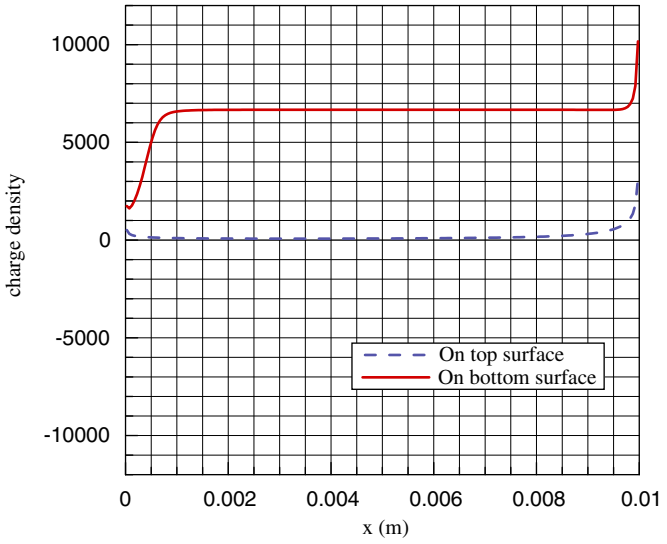

Fig. 8. Computed charge densities on the top beam surfaces (Fig. 6).

are added into the model, the number of elements along the beam length will be increased to 400.

Fig. 7 shows the computed charge densities on the center beam (beam 1) with positive voltage and the beam just below the center beam (beam 2) with negative voltage, for the model with 17 beams shown in Fig. 6. Due to the symmetry of the fields above and below each beam, the charge densities on the top and bottom surfaces of each beam are identical and thus only one field is plotted for each beam. The charge density on the two beams are also with the opposite sign and "anti-symmetrical", as expected. Fig. 8 is a plot of the charge densities on the bottom surface (σ^-) and top surface (σ^+) of the outer most (top) beam in Fig. 6. This plot is similar to the plot in Fig. 4 for the two parallel beam (with offset) case. It should be noted that the fields in MEMS are much more complicated than those that the simple parallel beam models can represent, especially near the edges of the beams, due to the simplified geometries used in this study. Nevertheless, the BEM code developed in this study can handle more complicated geometries of 2-D comb-drive models.

All the comb-drive models studied are summarized in Table 2. The parameters for each beam and gap are the same and the problem size is increased only by adding more beams in the model. Due to the memory limitation, the conventional BEM approach (with dual BIE (b)) can only handle models with elements up to 10,000 on the PC. The fast multipole BEM, however, can not only reduce the memory requirement, but also run much faster compared with the conventional BEM. Fig. 9 shows the CPU time comparison using the conventional BEM and the fast multipole BEM in solving these simple comb-drive models. As expected, the fast multipole BEM with the dual BIE (b) converges faster than the one with the regular BIE, due to the better conditioning of the dual BIE (b) formulation. The fast multipole BEM results converge in about 30–70

Table 2
Comparison of the CPU time for the conventional and fast multipole BEM

Comb-drive models			CPU time (s)		
Number of beams	Elements per beam	Total DOFs	Conventional BEM with dual BIE (b)	Fast multipole BEM with regular BIE	Fast multipole BEM with dual BIE (b)
5	410	2050	17.7	10.0	7.4
9	410	3690	92.5	33.0	18.9
13	410	5330	262.3	53.0	43.2
17	410	6970	569.9	64.0	43.1
21	410	8610	1067.1	76.0	53.0
25	410	10,250	1779.0	156.0	86.9
29	410	11,890	—	215.0	115.5
29	810	23,490	—	309.0	186.5
37	810	29,970	—	656.0	389.7
53	810	42,930	—	648.0	468.6
69	810	55,890	—	1421.0	918.5
85	810	68,850	—	2209.3	1236.9
125	810	101,250	—	2687.1	1979.5

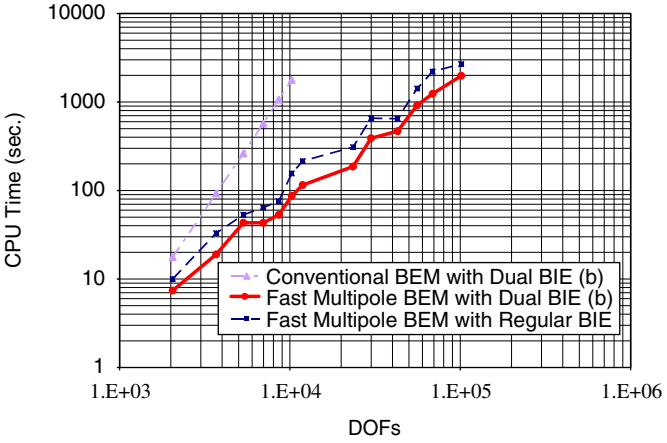

Fig. 9. CPU time for the conventional BEM and fast multipole BEM.

iterations using the dual BIE (b) and in about 50 to more than 100 iterations using the regular BIE.

It is evident from these preliminary studies that the dual BIE (b) is very effective in solving MEMS problems with thin beams and the fast multipole BEM using the dual BIE (b) is very efficient in solving large-scale models.

5. Discussions

Three electrostatic BIE formulations for modeling MEMS problems with thin beams are investigated, namely, the regular BIE in Eq. (4), the dual BIE (a) using the regular BIE on one surface of a beam and the gradient BIE (Eq. (5)) on the other surface, and the dual BIE (b) using a linear combination of the regular BIE and gradient BIE (Eq. (7)) on all surfaces of a beam. It is found that the regular BIE can handle thin beams with the thickness to length ratio h/L as small as 10^{-8}, when all the integrals are calculated analytically, while the dual BIE (a) and (b) can handle thin beams with h/L as small as 10^{-14} and 10^{-16}, respectively. However, both regular BIE and dual BIE (a) yield very high condition numbers for the systems of equations, and their accuracy and reliability for beams with very small thickness are in question. The dual BIE (b) yields relatively small condition numbers for beams with all the thickness studied and thus is a better candidate for implementation with the fast multipole BEM.

The fast multipole BEM is implemented for both the regular BIE and dual BIE (b) formulations based on the fast multipole BEM code presented in Ref. [30]. The treatment of the F kernel integral in gradient BIE (5) in the fast multipole expansions, which is not provided in Ref. [30], is also discussed. Simplified comb-drive models with increasing numbers of the beams are studied using the developed fast multipole BEM code. The results clearly demonstrate the potentials of the fast multipole BEM, especially, the one based on the dual BIE (b), for analyzing MEMS models with thin beams in a wide range of the thickness values.

More research needs to be done to improve the fast multipole BEM for modeling MEMS problems. More realistic MEMS models need to be studied to further test the developed code. Convergence of the solutions may be improved with better pre-conditioners. Fast multipole BEM code for analyzing 3-D electrostatic models need to be developed. Furthermore, coupled electro-mechanical analysis, dynamic and nonlinear problems can also be investigated.

Acknowledgments

This research has been supported by Grant CMS-0508232 of the US National Science Foundation. The author would also like to thank Professor Subrata Mukherjee at Cornell University for many helpful discussions on modeling MEMS problems with the BEM.

References

[1] Mukherjee S. Boundary element methods in creep and fracture. New York: Applied Science Publishers; 1982.
[2] Cruse TA. Boundary element analysis in computational fracture mechanics. Dordrecht, The Netherlands: Kluwer Academic Publishers; 1988.
[3] Brebbia CA, Dominguez J. Boundary elements—an introductory course. New York: McGraw-Hill; 1989.
[4] Banerjee PK. The boundary element methods in engineering. 2nd ed. New York: McGraw-Hill; 1994.
[5] Kane JH. Boundary element analysis in engineering continuum mechanics. Englewood Cliffs, NJ: Prentice-Hall; 1994.
[6] Shi F, Ramesh P, Mukherjee S. Simulation methods for micro-electro-mechanical structures (MEMS) with application to a micro-tweezer. Comput Struct 1995;56(5):769–83.
[7] Ye W, Mukherjee S. Optimal shape design of three-dimensional MEMS with applications to electrostatic comb drives. Int J Numer Methods Eng 1999;45:175–94.
[8] Ye W, Mukherjee S. Design and fabrication of an electrostatic variable gap comb drive in micro-electro-mechanical systems. CMES: Comput Modeling Eng Sci 2000;1(1):111–20.
[9] Shi F, Ramesh P, Mukherjee S. Dynamic analysis of micro-electro-mechanical systems (MEMS). Int J Numer Methods Eng 1996;39(24): 4119–39.
[10] Aluru NR, White J. An efficient numerical technique for electro-mechanical simulation of complicated microelectromechanical structures. Sensors Actuators A: Phys 1997;58(1):1–11.
[11] Bao Z, Mukherjee S. Electrostatic BEM for MEMS with thin conducting plates and shells. Eng Anal Boundary Elements 2004; 28(12):1427–35.
[12] Bao Z, Mukherjee S. Electrostatic BEM for MEMS with thin beams. Commun Numer Methods Eng 2005;21:297–312.
[13] De SK, Aluru NR. Full-Lagrangian schemes for dynamic analysis of electrostatic MEMS. J Microelectromech Syst 2004;13(5):737.
[14] Chyuan S-W, Liao Y-S, Chen J-T. Computational study of the effect of finger width and aspect ratios for the electrostatic levitating force of MEMS combdrive. J Microelectromech Syst 2005;14(2): 305–12.
[15] Rokhlin V. Rapid solution of integral equations of classical potential theory. J Comput Phys 1985;60:187–207.
[16] Greengard LF, Rokhlin V. A fast algorithm for particle simulations. J Comput Phys 1987;73(2):325–48.
[17] Greengard LF. The rapid evaluation of potential fields in particle systems. Cambridge: The MIT Press; 1988.
[18] Nishimura N. Fast multipole accelerated boundary integral equation methods. Appl Mech Rev 2002;55(4):299–324.
[19] Ljung P, Bachtold M, Spasojevic M. Analysis of realistic large MEMS devices. CMES: Comput Modeling Eng Sci 2000;1(1): 21–30.
[20] Frangi A, Gioia AD. Multipole BEM for the evaluation of damping forces on MEMS. Comput Mech 2005;37(1):24–31.
[21] Frangi A. A fast multipole implementation of the qualocation mixed-velocity-traction approach for exterior Stokes flows. Eng Anal Boundary Elements 2005;29(11):1039–46.
[22] Masters N, Ye W. Fast BEM solution for coupled 3D electrostatic and linear elastic problems. Eng Anal Boundary Elements 2004;28(9): 1175–86.
[23] Ding J, Ye W. A fast integral approach for drag force calculation due to oscillatory slip stokes flows. Int J Numer Methods Eng 2004;60(9): 1535–67.
[24] Frangi A, Tausch J. A qualocation enhanced approach for Stokes flow problems with rigid-body boundary conditions. Eng Anal Boundary Elements 2005;29(9):886.
[25] Liu YJ, Rudolphi TJ. Some identities for fundamental solutions and their applications to weakly-singular boundary element formulations. Eng Anal Boundary Elements 1991;8(6):301–11.

[26] Krishnasamy G, Rizzo FJ, Liu YJ. Boundary integral equations for thin bodies. Int J Numer Methods Eng 1994;37:107–21.
[27] Liu YJ, Rizzo FJ. Scattering of elastic waves from thin shapes in three dimensions using the composite boundary integral equation formulation. J Acoust Soc Am 1997;102(2, Part 1):926–32.
[28] Burton AJ, Miller GF. The application of integral equation methods to the numerical solution of some exterior boundary-value problems. Proc R Soc London A 1971;323:201–10.
[29] Liu YJ, Rizzo FJ. A weakly-singular form of the hypersingular boundary integral equation applied to 3-D acoustic wave problems. Comput Methods Appl Mech Eng 1992;96:271–87.
[30] Liu YJ, Nishimura N. The fast multipole boundary element method for potential problems—a tutorial. Eng Anal Boundary Elements 2006;30:371–81.
[31] Hayt WH, Buck JA. Engineering electromagnetics. London: McGraw Hill; 2001.